

Constraining vectors and axial-vectors in walking technicolour by a holographic principle

Dennis D. Dietrich

*HEP Center, Institute for Physics and Chemistry,
University of Southern Denmark, Odense, Denmark*

Chris Kouvaris

The Niels Bohr Institute, Copenhagen, Denmark

(Dated: July 16, 2008)

We use a holographic principle to study the low-energy spectrum of walking technicolour models. In particular, we predict the masses of the axial vectors as well as the decay constants of vectors and axial vectors as functions of the mass of the techni- ρ . Given that there are very few nonperturbative techniques to study strongly coupled theories, using holography might provide us with insight into how to constrain the parameters of the low-energy effective action of walking technicolour models. We also compare our results with findings from other setups.

PACS numbers: 12.60.Nz, 11.25.Tq, 12.40.-y, 12.40.Yx, 11.15.Tk

I. INTRODUCTION

The standard model is remarkably consistent with currently available data for the interactions of elementary particles, but it has some theoretical shortcomings. First of all, although the existence of the (still elusive) fundamental Higgs scalar is essential for the standard model in order to account for the spontaneous breaking of the electroweak symmetry, nature has shown no preference for fundamental scalars in analogous cases. In the well known examples of superconductivity and superfluidity, the corresponding scalars turn out to be composite objects kept together by intricate strong dynamics. Apart from this aesthetically unappealing feature of the standard model, there are more serious problems, like the instability of the Higgs scalar's mass with respect to quantum corrections which necessitates fine tuning also referred to as the hierarchy problem. There exists a number of extensions of the standard model which tries to overcome these deficiencies. The one we are concerned with here is called technicolour [1]. In technicolour the spontaneous breaking of the electroweak symmetry is not due to an elementary scalar Higgs particle acquiring a vacuum expectation value. Instead, the standard model without elementary scalar is supplemented with an additional strongly interacting sector such that chiral symmetry breaking among the so-called techniquarks breaks the electroweak symmetry down to the electromagnetic gauge group. From the experimental point of view, the low-energy spectrum of such a sector is most accessible and therefore most relevant. The corresponding degrees of freedom can be encoded in an effective Lagrangian which is constructed such that it reflects the symmetries—gauge and flavour—of the underlying theory. In general, for a given theory, the effective Lagrangian features a large number of parameters. Linking the effective Lagrangian directly to the elementary theory is a non-trivial task. In QCD where this approach

is also followed, fitting to experimental data permits to give values to aforementioned parameters. In the absence of data, and that, for the time being, is the situation in the case of technicolour, this is not an option and other principles have to be devised.

Walking [2], that is quasi-conformal technicolour theories with techniquarks in higher dimensional representations are compatible with currently available precision data [3]. In the following, we will study those walking technicolour models which in the survey [4] have been identified as viable candidates for breaking the electroweak symmetry dynamically. In particular, we will concentrate on the prime candidate, usually referred to as minimal walking technicolour. It consists of two techniflavours transforming under the adjoint representation of an $SU(2)$ technicolour gauge group. As the adjoint representation of $SU(2)$ is real, this model features an enhanced flavour symmetry $SU(4)$ instead of the $SU(N_f) \times SU(N_f)$ for non-(pseudo)real representations. Assuming a breaking to the minimal diagonal subgroup, the $SU(4)$ breaks to $SO(4)$ which leads to nine Goldstone modes. This fact together with the enlarged vector and axial vector meson sector leads to a rich low-energy effective theory [5, 6].

There are different ways to constrain the parameter space of the effective Lagrangian. In [7], the authors employ Weinberg's sum rules [8] for this purpose: Counting the expression for the oblique S parameter [9] as zeroth sum rule, the perturbative expression obtained for the elementary theory and the value computed on the low-energy side are postulated to be equal. Further, the first sum rule is imposed for the respective first resonances. Likewise, the second, for which also modifications due to the continuum are taken into account [10] ¹.

¹ In the strict sense this does not reduce the number of free parameters, but introduces a new one. Over the latter, however,

Here, we impose a holographic principle—the details of which will be laid out in the next section—motivated by the AdS/CFT correspondence [11]. It maps a five-dimensional gravity theory onto a four-dimensional conformal field theory. Originally, the AdS/CFT correspondence has been conjectured for $\mathcal{N} = 4$ supersymmetry which is an exactly conformal theory. Its application to non-conformal theories has to be interpreted as extrapolation. Astonishingly enough, however, holographic descriptions of QCD give results of remarkably good agreement with experiments [12, 13]. Currently, holography is used extensively as a mathematical tool to probe aspects of nonperturbative QCD, either in quark-gluon plasma [14] or hadronic physics [15]. The scale invariance in QCD is broken due to quantum effects and nonzero quark masses. The success of the holographic principle in QCD might probably be attributed to the fact that for energies below 1 GeV, the strong coupling constant effectively behaves as constant. Lattice simulations support the possibility of an infrared fixed point [16, 17]. In the case of technicolour, walking models are by construction quasi-conformal, where the coupling changes only slightly between the electroweak scale and the scale of the extended theory which should be larger than at least 300 times the electroweak. Therefore they meet the criteria for applying holography in a much better way than QCD does [18]. Higher-dimensional holographic frameworks have even been used as basis for the construction of technicolour-like models [19]. One should not take for granted the findings of the holographic description, but holography remains one of the very few mathematical tools in the arsenal of theoretical physics for the study of strongly coupled theories. Recently, also lattice methods have been implemented for the study of the dynamics of minimal walking technicolour [20, 21]. By using different methods, what one could certainly achieve is a test of the robustness of investigated features with respect to different setups. Within the holographic approach, additional choices must be made, like, for example for boundary conditions. With the interpretation of the fifth dimension as inverse energy scale, there are two very general types of boundary conditions we impose. Below, we will compare a hard-wall approach [12, 22], that is the fifth dimension z is limited to a finite interval between two values ϵ and z_m that correspond to the ultraviolet and infrared scales of the theory, respectively, and a soft-wall approach [23], where, although z can go to infinity, there is a potential term that effectively works as a form factor, smoothing out the sharp boundary of the hard-wall model. For QCD the latter is phenomenologically favoured as it is able to reproduce the Regge trajectories for the vector resonances. Due to the absence of the corresponding data there is no such criterion for the quasi-conformal theories we are concerned with, and ad-

ditionally, here we concentrate on the lowest lying vector and axial-vector resonance, respectively. Therefore, we compare the two corresponding results on an equal footing.

In Sect. II, we describe the underlying holographic principle, derive the equations of motion relevant for the treatment of the spectrum of walking technicolour theories, and give the necessary solutions. In Sect. III, we continue by analysing the obtained quantitative results and discuss their phenomenological implications. In Sect. IV, we summarise our findings.

II. HOLOGRAPHIC APPROACH

We will here employ modifications of the five-dimensional holographic models used in [12, 18, 23]. In their primary form, that is for a $SU(N_f) \times SU(N_f)$ flavour symmetry they are based on the action,

$$S := \int d^5x \sqrt{g} \mathcal{L} \quad (1)$$

$$\mathcal{L} := \text{tr} [|D\Phi|^2 + m_5^2 |\Phi|^2 - \frac{1}{4g_5^2} (F_L^2 + F_R^2)]. \quad (2)$$

The metric is to be anti de Sitter,

$$ds^2 = z^{-2} (-dz^2 + dx^2), \quad (3)$$

with the interpretation of the fifth coordinate, z , as inverse energy scale. The basic idea is to gauge the global group $SU(N_f) \times SU(N_f)$ in the five dimensional theory. The left, $A_{L,\mu}^a \doteq \bar{q}_L \gamma_\mu t^a q_L$, and the right $A_{R,\mu}^a \doteq \bar{q}_R \gamma_\mu t^a q_R$, vector fields, appear in the covariant derivative coupling to the scalar Φ , $D_\mu \Phi := \partial_\mu \Phi - iA_{L\mu} \Phi + i\Phi A_{R\mu}$, as well as in the left and right field tensors, $F_{\mu\nu} := \partial_\mu A_\nu - \partial_\nu A_\mu - i[A_\mu, A_\nu]$. $q_{L/R}$ stand for the left-/right-handed techni-quarks. Here, t^a are the generators of the flavour symmetry group. The scalar field $\Phi^{\alpha\beta}$ corresponds to the scalar combination of techni-quarks $\bar{q}_R^\alpha q_L^\beta$.² By matching to perturbative calculations the coupling g_5 is identified with,

$$g_5^2 = 12\pi^2/d_R, \quad (4)$$

where d_R is the dimension of the representation of the technicolour gauge group under which the techni-quarks transform.

From the action (1), one obtains the equation of motion for the scalar expectation value Φ_0 which breaks the chiral symmetry,

$$[z^3 \partial_z z^{-3} \partial_z - z^{-2} m_5^2] \Phi_0 = 0. \quad (5)$$

one has more quantitative control.

² The case where we have the techni-quarks transforming under a (pseudo)real representation of the gauge group is slightly different because of an enhanced global symmetry and is discussed in subsection C.

With the ansatz $\Phi_0 \sim z^d$, one finds the characteristic equation

$$m_5^2 = d(d-4). \quad (6)$$

d is equal to the dimension of the scalar operator on the boundary. For a quasi-conformal theory we set $d = 2$, hence, $m_5^2 = -4$. The solution for Φ_0 is

$$\Phi_0 = c_1 z^2 + c_W z^2 \ln(z/\epsilon), \quad (7)$$

where c_1 and c_W should be fixed by boundary conditions. The ultraviolet boundary condition is $(2/\epsilon)\Phi_0(\epsilon) = M$, where M is the techniquark mass matrix. From this condition, in the chiral limit ($M = 0$), we get $c_1 = 0$. The other constant c_W will be fixed later on, once we adjust the technipion decay constant f_π to the electroweak scale.

The equations of motion for the vector meson, $2V := A_L + A_R$, is extracted from the terms of the action (1) quadratic in these fields. In the $V_z = 0$ gauge and after having Fourier transformed all space-time coordinates except z , V satisfies,

$$[z\partial_z z^{-1}\partial_z + q^2]V = 0. \quad (8)$$

Similarly, for the transverse part of the axial vector meson fields, $2A := A_L - A_R$,

$$[z\partial_z z^{-1}\partial_z + q^2 - g_5^2 z^{-2}\Phi_0^2]A = 0, \quad (9)$$

which couple to the scalar expectation value Φ_0 . For the sake of getting analytic results and with negligible loss of accuracy, we approximate $\Phi_0 = c_W z^2 \ln(z/\epsilon) \simeq c_W z^2 \ln(z_m/\epsilon)$. This approximation works well: For the hard-wall approach which we are going to discuss next, z is confined (as we already mentioned) between ϵ and z_m . The approximation we make is worst for small z , close to ϵ , and it gets really good for large z , close to z_m . From Eq. (9), we see that the last term of the equation is negligible close to the ultraviolet boundary. This means that the term we approximate can be neglected where the approximation is not accurate; where it becomes important (close to the infrared boundary), the approximation is extremely accurate. The same happens for the soft-wall approach, although, z can in principle assume arbitrarily large values, the potential term will effectively cut it off smoothly. As we shall argue, there is no need to specify a value for z_m for the approximation to work because the factor $\ln(z_m/\epsilon)$ is just a constant and can be absorbed in c_W . Φ_0 from Eq. (7) can be written as,

$$\Phi_0 \approx C z^2 / g_5. \quad (10)$$

Thus, in the hard-wall model to be discussed next, $C \approx g_5 c_W \ln(z_m/\epsilon)$.

A. Hard-wall model

As mentioned before, in the hard-wall approach z is confined between ϵ and z_m . Concretely, for the vector V

and axial vector A , the wave functions satisfy the boundary conditions [12],

$$V(\epsilon) = 0 = \partial_z V(z_m), \quad (11)$$

$$A(\epsilon) = 0 = \partial_z A(z_m). \quad (12)$$

z_m characterises the position of the infrared boundary, ϵ that of the ultraviolet boundary. For quasi-conformal theories, that is theories which feature almost conformal behaviour over an interval of scales, the two aforementioned points along the fifth dimension can be seen as the boundaries of this interval [18]. For phenomenologically viable technicolour models $\epsilon \ll z_m$. To be more precise z_m/ϵ should be at least 300, with 1000 being probably a typically expected value [24]. We can, hence, go to the limit $\epsilon \rightarrow 0$ which turns out to be smooth and not to have an important quantitative impact.

The pion decay constant f_π can be obtained from the solution of the axial-vector equation of motion for $q^2 = 0$ and with the boundary conditions,

$$\partial_z \mathcal{A}(z_m) = 0 \quad \text{and} \quad \mathcal{A}(0) = 1. \quad (13)$$

It is given by,

$$g_5^2 f_\pi^2 = -\partial_z^2 \mathcal{A}(0), \quad (14)$$

which arises from $-\epsilon^{-1}\partial_z \mathcal{A}(\epsilon)$ in the limit $\epsilon \rightarrow 0$ because $\partial_z \mathcal{A}(0) = 0$. The general solution for the vectorial equation of motion is given by a linear combination of the Bessel functions of order one $J_1(qz)$ and $Y_1(qz)$ both multiplied by z . Only $zJ_1(qz)$ satisfies the boundary condition at $z = 0$. The boundary condition at $z = z_m$ implies,

$$J_0(qz_m) = 0, \quad (15)$$

which represents an eigenvalue equation for q . Thus, the mass of the lightest vector resonance, the techni- ρ , is given by,

$$M_V = 2.4048/z_m, \quad (16)$$

where the numerator is given by the first zero of J_0 .

The axial equation of motion is solved by linear combinations of $z^2 e^{-Cz^2/2}$ times the Kummer functions (confluent hypergeometric functions) $M(1 - \frac{q^2}{4C}, 2, Cz^2)$ and $U(1 - \frac{q^2}{4C}, 2, Cz^2)$. The boundary condition at $z = 0$ eliminates contributions involving the function U . Then the boundary condition at $z = z_m$ leads to the eigenvalue equation,

$$(2C^2 z_m^2 - M_A^2)M(1 - \frac{M_A^2}{4C}, 2, Cz_m^2) + (4C + M_A^2)M(-\frac{M_A^2}{4C}, 2, Cz_m^2) = 0, \quad (17)$$

which can only be evaluated numerically.

The differential equation for \mathcal{A} possesses solutions made up of hyperbolic functions, $\sinh(Cz^2/2)$ and $\cosh(Cz^2/2)$. The boundary condition at $z = 0$ fixes

the prefactor for the cosh term to 1. Exploiting the expression arising from the boundary condition at $z = z_m$ leads to,

$$\mathcal{A} = \cosh(Cz^2/2) - \tanh(Cz_m^2/2) \sinh(Cz^2/2). \quad (18)$$

Evaluation of Eq. (14) for this solution yields,

$$g_5^2 f_\pi^2 = C \tanh(Cz_m^2/2). \quad (19)$$

The decay constants of the vector and the axial vector are obtained from

$$g_5 F_V = \partial_z^2 V(0), \quad (20)$$

$$g_5 F_A = \partial_z^2 A(0), \quad (21)$$

where V and A have to be normalised according to,

$$\int_0^{z_m} \frac{dz}{z} V^2 = 1 = \int_0^{z_m} \frac{dz}{z} A^2. \quad (22)$$

The normalised vectorial solution reads,

$$V = \sqrt{2} \frac{z J_1(M_V z)}{z_m J_1(M_V z_m)}, \quad (23)$$

and leads to the decay constant,

$$g_5 F_V = 1.1328 M_V^2, \quad (24)$$

where the expression has been evaluated at the first zero of J_0 . The normalisation integral for A must be evaluated numerically.

B. Soft-wall model

In [23] an additional dilaton field ϕ is introduced into the action,

$$S_s := \int d^5 x \sqrt{g} e^{-\phi} \mathcal{L}. \quad (25)$$

Requiring that the mass spectrum show a Regge like spacing linear in the squared mass, the dilaton background should behave like cz^2 ($c = \text{constant}$) for large values of z . Compared to the potential well of the hard-wall model, this leads to a harmonic oscillator like setting which in turn gives linearly spaced eigenvalues for the squared mass.

Rederiving the vectorial equation of motion yields,

$$[ze^{+cz^2} \partial_z z^{-1} e^{-cz^2} \partial_z + q^2] V_s = 0, \quad (26)$$

and the infrared boundary condition is replaced by postulating the normalisability of the solution over \mathbb{R}^+ . With the substitution,

$$V_s =: v_s e^{+cz^2/2}, \quad (27)$$

v_s obeys the equation of motion,

$$[z \partial_z z^{-1} \partial_z + q^2 - c^2 z^2] v_s = 0, \quad (28)$$

and must satisfy the same boundary condition as V_s . The differential equation for v_s coincides with that for A in the hard-wall case, up to the interchange of the constants c and C . Therefore, the solution for v_s with the correct behaviour at the UV boundary has already been given in the previous section in the context of the axial vector wave function. The aforementioned normalisability of the solution implies that the eigenvalues M_V^2 be integer multiples of $4c$. (For these values the Kummer function M turns into a polynomial.)

Before we can continue with the axial vector mesons, we have to know the expectation value Φ_s for the scalar. The relevant equation of motion is given by,

$$[z^3 e^{+cz^2} \partial_z z^{-3} e^{-cz^2} \partial_z + z^{-2} m_s^2] \Phi_s = 0. \quad (29)$$

With a substitution,

$$\Phi_s =: \varphi_s e^{+cz^2/2}, \quad (30)$$

which leads to the same boundary condition for φ_s as for Φ_s , the previous differential equation turns into,

$$[z^3 \partial_z z^{-3} \partial_z + z^{-2} m_s^2 - c^2 z^2] \varphi_s = 0. \quad (31)$$

For $c^2 z^4 \ll m_s^2$ the characteristic equation (6) holds to good approximation and through identification in the ultraviolet we can again set $m_s^2 = -4$. The solution for the previous equation is then given by linear combinations of z^2 times the Bessel functions $I_0(cz^2/2)$ and $K_0(cz^2/2)$. (For $m_s^2 \neq -4$ the order of the Bessel functions changes.) The boundary condition $\lim_{\epsilon \rightarrow 0} \Phi_s(\epsilon) = 0$ and equivalently $\lim_{\epsilon \rightarrow 0} \varphi_s(\epsilon) = 0$ selects the solution,

$$\varphi_s = c_s z^2 I_0(cz^2/2). \quad (32)$$

Already φ_s exhibits exponential growth for large values of z and moreso does Φ_s with its additional exponential factor. This observation is indicative of an instability which must eventually be intercepted by non-linear terms in the equation of motion which would originate from potential terms involving the (pseudo)scalar fields [23]. At the linear level we have to adhere to small values of z and we can use henceforth,

$$\varphi_s = c_s z^2 [1 + O(c^2 z^4/4)]. \quad (33)$$

Φ_s contains an additional exponential factor. As we are confined to small values of z in any case and for the sake of an analytical result we approximate it by unity,

$$\Phi_s = c_s z^2 [1 + O(cz^2/2)]. \quad (34)$$

This is the dominant approximation and we shall determine its range of applicability below.

The equation of motion for the wave function of the axial vector mesons reads,

$$[ze^{+cz^2} \partial_z z^{-1} e^{-cz^2} \partial_z + q^2 - g_5^2 z^{-2} \Phi_s^2] A_s = 0, \quad (35)$$

where Φ_s is the expectation value for the scalar. As above, we carry out the substitution,

$$A_s = a_s e^{+cz^2/2}, \quad (36)$$

which leads to,

$$[z\partial_z z^{-1}\partial_z + q^2 - c^2 z^2 - g_5^2 z^{-2}\Phi_s^2]a_s = 0, \quad (37)$$

and does not affect the boundary conditions.

Using the dominant term from Eq. (34), we end up with the following equation of motion for a_s ,

$$\{z\partial_z z^{-1}\partial_z + [q^2 - (c^2 + C^2)z^2]\}a_s = 0. \quad (38)$$

Up to the replacement of c^2 by $c^2 + C^2$, it coincides with the equation of motion for v_s . The boundary condition is the same. Thus, the corresponding solution can be obtained by carrying out the aforesaid replacement. Accordingly, requiring the normalisability of the wave function implies that the squared mass eigenvalues M_A^2 be integer multiples of $4\sqrt{c^2 + C^2}$.

Finally, we would like to extract the pion decay constant from the solution of the axial differential equation with $q^2 = 0$,

$$(ze^{+cz^2}\partial_z z^{-1}e^{-cz^2}\partial_z - C^2 z^2)\mathcal{A}_s = 0, \quad (39)$$

or

$$[z\partial_z z^{-1}\partial_z - (c^2 + C^2)z^2]\mathcal{A}_s = 0, \quad (40)$$

where,

$$\mathcal{A}_s =: \mathbb{A}_s e^{+cz^2/2}. \quad (41)$$

Replacing C by $\sqrt{C^2 + c^2}$ in Eq. (18) and sending z_m to infinity yields,

$$\mathbb{A}_s = e^{-z^2\sqrt{C^2 + c^2}/2}, \quad (42)$$

or

$$\mathcal{A}_s = e^{-z^2(\sqrt{C^2 + c^2} - c)/2}. \quad (43)$$

Hence, from Eq. (14),

$$g_5^2 f_\pi^2 = \sqrt{C^2 + c^2} - c. \quad (44)$$

Using the previous results on the mass eigenvalues we find,

$$M_A^2 = M_V^2 + 4g_5^2 f_\pi^2. \quad (45)$$

(For the n^{th} pair of resonances this relation turns into $M_{A,n}^2 = M_{V,n}^2 + 4ng_5^2 f_\pi^2$.)

In order to extract the decay constants for the vector and axial vector mesons it remains to normalise the corresponding wave functions according to,

$$\int_0^\infty \frac{dz}{z} v_s^2(z) = 1 = \int_0^\infty \frac{dz}{z} a_s^2(z). \quad (46)$$

With $M_V^2 = 4c$ the normalised wave function for the vector reads,

$$V_s = \sqrt{2}cz^2. \quad (47)$$

The decay constant equals,

$$g_5 F_V = \partial_z^2 V_s(0) = 2\sqrt{2}c = M_V^2/\sqrt{2}. \quad (48)$$

With a prefactor of 0.707... the rise of F_V with M_V^2 is shallower than in the hard-wall model, where the prefactor was approximately 1.133. Similarly, the results for the axial vector are,

$$A_s = \sqrt{2}\sqrt{c^2 + C^2}z^2, \quad (49)$$

and

$$g_5 F_A = \partial_z^2 A_s(0) = 2\sqrt{2}\sqrt{c^2 + C^2} = M_A^2/\sqrt{2}. \quad (50)$$

As already announced, we are now going to assess the range of applicability of the approximations carried out above. The approximation introducing an $O(cz^2)$ deviation was replacing the additional exponential in Eq. (30) by unity. In the spirit of perturbation theory, we now calculate the shift δq^2 of M_A^2 induced by the perturbation, that is the difference between the exact and the approximated potential. For this we need to know the normalised wave function,

$$a_s = \sqrt{2}\sqrt{c^2 + C^2}z^2 e^{-\sqrt{c^2 + C^2}z^2/2}, \quad (51)$$

and the perturbation of the potential,

$$\delta U := C^2 z^2 (e^{+cz^2} - 1). \quad (52)$$

The shift is then given by,

$$\begin{aligned} \delta q^2 &= \int_0^\infty \frac{dz}{z} a_s^2 \delta U = \\ &= 2C^2(C^2 + c^2) \times \\ &\quad \times [(\sqrt{C^2 + c^2} - c)^{-3} - (C^2 + c^2)^{-3/2}]. \end{aligned} \quad (53)$$

This quantity must be compared to $M_A^2 = 4\sqrt{c^2 + C^2}$ and should be smaller than the latter, implying that,

$$x^2 \sqrt{1+x^2} [(\sqrt{1+x^2} - 1)^{-3} - (1+x^2)^{-3/2}] \ll 2, \quad (54)$$

where $x := C/c$. The left-hand side of the previous expression diverges for small values of x and tends to zero for large values of x . Therefore, we must have $C \gg c$. With the help of Eq. (44) we can translate this into ranges for the vectorial mass M_V ,

$$x = \sqrt{(1+y^2) - y^2}/y, \quad (55)$$

where $y := c/(g_5^2 f_\pi^2)$. The previous expression tends to infinity for small values of y and to zero for large values

of y . We should, thus, keep y small. This corresponds to an upper bound on the vectorial mass, $M_V = 2\sqrt{c} \ll g_5 f_\pi$. For minimal walking technicolour this corresponds to roughly 1.5TeV. Without giving the details here, in the spirit of an iterative procedure, we have further improved the treatment of the soft-wall setting by calculating a new effective value for the parameter C by averaging the corresponding potential term with the initially obtained wave-function (51). Comparison of the initial with the thus obtained result shows that at very small M_A the two results coincide and that at $M_A \approx 1.5\text{TeV}$ the old result is ten percent lower than the new. For $M_A \approx 3\text{TeV}$ the results differ by a hundred percent.

C. Real and pseudo-real representations

For N_f techniquarks transforming under real or pseudo-real representations of the technicolour gauge group, the unbroken flavour symmetry is enhanced to $SU(2N_f)$. The $SU(N_f)_L \times SU(N_f)_R$ which has been treated up to this point is a subgroup of $SU(2N_f)$ and can be embedded in it. There will not only be the previous $2(N_f^2 - 1)$ (axial) vectors, but a total of $(2N_f)^2 - 1$, that is an extra $2N_f^2 + 1$. In the action they will have their own kinetic terms and they appear in the covariant derivative. Apart from new characteristics like non-zero technibaryon number, from the point of view of the flavour symmetry they are still either vector or axial vector eigenstates. Hence, if the unbroken flavour symmetry is an exact symmetry, they have the same masses as the standard vectors and axial vectors, respectively. If they couple to the condensate (axial eigenstate) or not (vectorial eigenstate) depends on whether the corresponding generator of the flavour symmetry group commutes with the condensate or not. Such a coincidence of values is also present for the decay constants of the states which can decay, that is the mesons. At the present level, technibaryon number is conserved, so that the baryonic modes cannot decay.

In order to give a concrete example, let us look at minimal walking technicolour, using the notation from [6]. There are two techniquarks, U and D , that transform under the adjoint representation of the $SU(2)$ technicolour group. As the adjoint of $SU(2)$ is a real representation, the global symmetry of the model is $SU(4)$. The flavour symmetry no longer only transforms left-fields, (U_L, D_L) , among themselves and right-fields, (U_R, D_R) , among themselves, but also left- into right-fields and vice versa. Therefore, it is practical to work in a joint basis, say

$$Q_j^\alpha = \begin{pmatrix} U_L \\ D_L \\ -i\sigma^2 U_R^* \\ -i\sigma^2 D_R^* \end{pmatrix}, \quad (56)$$

where Greek and Latin indices denote spin (α runs from 1 to 2) and flavour components, respectively. Let T^a

be a set of 15 generators for $SU(4)$ in the fundamental representation. Divide them into the first six, $S^a := T^a$, $a \in \{1; \dots; 6\}$, commuting with the condensate, which is to be proportional to a 4×4 matrix E , and the following nine, $X^a := T^{a+6}$, $a \in \{1; \dots; 9\}$, which do not commute with E . For

$$E = \begin{pmatrix} 0 & \mathbb{1} \\ \mathbb{1} & 0 \end{pmatrix}, \quad (57)$$

where $\mathbb{1}$ stands for the 2×2 unit matrix, the condensate is thus, $\langle Q_i^\alpha Q_j^\beta \epsilon_{\alpha\beta} E^{ij} \rangle = -2 \langle \bar{U}_R U_L + \bar{D}_R D_L \rangle$, where $\epsilon_{\alpha\beta}$ is the two-dimensional antisymmetric symbol. (For an explicit realisation for the generators see Appendix A of [6].) The covariant derivative for Φ in the action (1) is given by

$$D_\mu \Phi = \partial_\mu \Phi - i A_\mu \Phi - i \Phi A_\mu^\top, \quad (58)$$

where $A_\mu = A_\mu^a T^a$. $\Phi^{\alpha\beta}$ is also promoted to a 4×4 matrix, that now represents the techniquark combination $Q_i^\alpha Q_j^\beta \epsilon_{\alpha\beta}$. It should be noted that the above techniquark composite scalar contains the degrees of freedom associated with $\bar{q}_R^\alpha q_L^\beta$ known from the previous sections, exactly as $SU(4)$ contains $SU(2)_L \times SU(2)_R$ as subgroup. The $SU(2)_L \times SU(2)_R$ part can be embedded by defining the corresponding generators according to $\sqrt{2}L^a := X^a + S^a$ and $\sqrt{2}R^a := X^a - S^a$, where $a \in \{1; 2; 3\}$. The fields belonging to the generators S^4, S^5 , and S^6 lead to three additional eigenstates. In this special setting one of them is a meson and the other two an axial vector baryon and its antibaryon. The fields belonging to the six remaining generators X^4 to X^9 not commuting with the condensate correspond to three baryon-antibaryon pairs which are vector eigenstates. In addition to the three mesonic Goldstone modes arising from the broken axial $SU(2)$, there are six more, arranged in three baryon-antibaryon pairs. They have also to be included in the corresponding kinetic and mass terms. We assume zero mass for the techniquarks, and, therefore, there is no isospin splitting. Hence, the richer pseudoscalar sector does not influence the results at this level. What the decay constants of the technibaryonic states—spin zero as well as spin-one—are concerned, these states do not decay, as on this level technibaryon number is conserved³.

III. RESULTS AND DISCUSSION

A. Minimal walking technicolour

After fixing f_π to its phenomenological value of $246\sqrt{2/N_f}$ GeV, there is only one free parameter left

³ That is, conserved perturbatively. It can change through sphaleron processes which, however, are extremely suppressed [28].

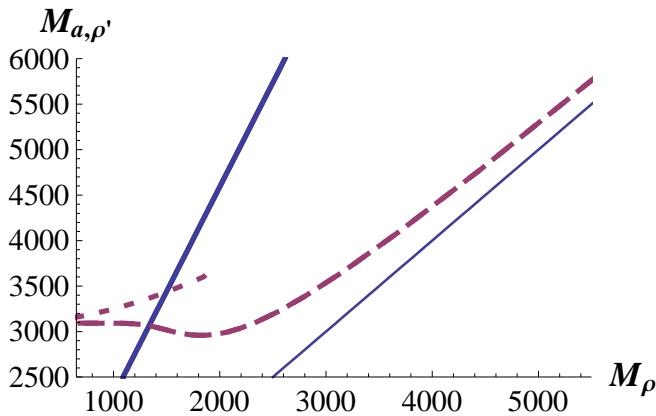


FIG. 1: Minimal walking technicolour: The mass M_a of the first axial vector meson as function of the mass M_ρ of the first vector meson in the hard-wall model (long dashes) and in the soft-wall model (short dashes). For comparison, the finer straight line indicates the diagonal $M_a = M_\rho$. The wider straight line indicates the mass $M_{\rho'}$ of the second vector resonance in the hard-wall model.

in the present approach. Consequently, the results can be presented as one-parameter curves. For minimal walking technicolour with its $N_f = 2$ flavours in the (three-dimensional) adjoint representation of $SU(2)$, $g_5^2 = 4\pi^2$.

The axial vector meson mass as a function of the vector meson mass is shown in Fig. 1. For small vector meson masses, the mass of the first axial vector state coincides in the two scenarios, hard- and soft-wall, respectively. The axial vector mass is bounded from below. The axial vector mass in the soft-wall model is a monotonously rising function of the vector mass and, hence, the minimum is reached for vanishing vector masses. It is given by,

$$M_a > 2g_5 f_\pi, \quad (59)$$

which here equals roughly 3 TeV. (From this point onward, we will use the subscript a for the lightest axial vector resonance and ρ for the lightest vector resonance. Likewise, ρ' indicates the corresponding first excitation.) In the hard-wall model, M_a starts out by first decreasing slightly when M_ρ is increased before increasing again. In both scenarios the axial vector mass then approaches the vector mass from above without ever falling below it. The axial vector mass in the soft-wall approach stays also always larger than the hard-wall approach. For a light first vector meson (M_ρ) also the second resonance ($M_{\rho'}$)—or even higher vector resonances—can be lighter than the first axial vector meson (see the bold straight line in Fig. 1).

In the soft-wall model, the decay constants both for the vector and the axial vector meson as functions of the respective mass show the same behaviour, that is linear for the square root of the decay constants (see Fig. 2). The same is true for the vector meson in the hard-wall model, albeit with a different slope. For the hard-wall model the decay constant of the axial vector shows a

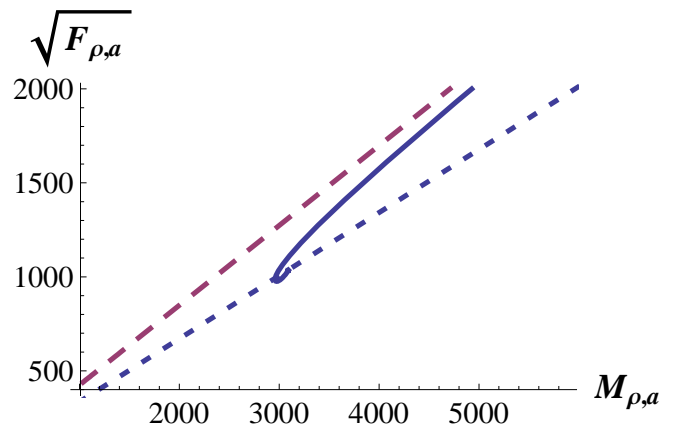


FIG. 2: Minimal walking technicolour: The square-root of the decay constant of the first vector meson $\sqrt{F_\rho}$ as function of its mass M_ρ (hard-wall: long dashes, soft-wall: short dashes) and the square-root of the decay constant of the first axial vector meson $\sqrt{F_a}$ as function of its mass M_a (hard-wall: solid line, soft-wall: short dashes) for the hard- and the soft-wall model, respectively. The hook-like structure in the axial vector graph is linked to the non-monotonous behaviour of M_a as a function of M_ρ in the hard-wall model (see Fig. 1). In the soft-wall model the graphs for the vector and axial vector coincide. Remember, however, that there the approximations made for the *axial* vector are only valid for small masses.

different behaviour. For increasing mass, it approaches the vectorial behaviour from below. At small values of the mass the axial vector decay constant in the hard-wall model is numerically closer to the outcome of the soft-wall scenario. This is understandable as for large masses in the hard-wall scenario the spacing between the infrared and the ultraviolet wall is rather small and the tilting of the floor of the square-well potential by the condensate for the axial vector as opposed to the flat bottom for the vector does not play a prominent role. For small masses the infrared wall is approximately infinitely far away and the axial behaves like in the soft-wall case. This is also the reason why its mass does not go down to arbitrarily small values in either scenario.

The setup laid out in Ref. [6], contains additional terms coupling scalar operators to the spin-one fields not present in the holographic approach pursued here. {See, for example, Eq. (41) in Ref. [6].} This is chiefly due to the fact that there the spin-one fields are associated with the *global* flavour symmetry. This allows for more invariant terms than if the field is associated with a *local* symmetry as is the case in a holographic setting. A non-minimal term, which is also locally invariant is $\text{tr}(F_{\mu\nu}\Phi F^{\mu\nu\top}\Phi^\dagger)$ [27]. The higher number of parameters allows for a more diverse phenomenology than seen in the present, more (and differently) constrained approach. Most prominently, the axial vector meson may also be lighter than the vector meson, in contrast to the present findings. Here, the axial is found to have a mass of ~ 3 TeV and above. In this range also the mass hierarchy

N_c	representation	d_R	N_f	N_f^g	$M_{a,\text{soft}}^{\text{min}}$	$(F_a^{\text{min}})^{1/2}$
2	fundamental	2	7	6	2.2	0.66
2	fundamental	2	7	2	3.8	1.15
2	adjoint	3	2	2	3.1	1.04
3	fundamental	3	11	2	3.1	1.04
3	2-ind.sym.	6	2	2	2.2	0.87
3	adjoint	8	2	2	1.9	0.81
4	fundamental	4	15	2	2.7	0.97
4	2-ind.sym.	10	2	2	1.7	0.77
4	2-ind.antisym.	6	8	2	2.2	0.87
4	adjoint	15	2	2	1.4	0.69
5	fundamental	5	19	2	2.4	0.91
5	2-ind.antisym.	10	6	2	1.7	0.77
6	fundamental	6	23	2	2.2	0.87

TeV TeV

TABLE I: Various walking technicolour models from Tab. III in [4]. Minimal axial vector meson mass $M_{a,\text{soft}}^{\text{min}}$ and square-root of the minimal axial decay constant $(F_a^{\text{min}})^{1/2}$ for various walking technicolour models characterised by the representation of the technicolour gauge group under which the techniquarks transform and the number of (gauged) techniflavours N_f (N_f^g).

in Ref. [7] is the one known from quantum chromodynamics with the lighter vector. Our Eq. (45) is directly reminiscent of Eq. (C8) in Ref. [6]. This allows us to compare our $\sqrt{C^2 + c^2} - c$ to their $v^2 \tilde{g}^2 r_2 / 8$. There v^2 stands for the strength of the chiral condensate, \tilde{g} represents the coupling constant for the (axial) vector fields, and r_2 parametrises the relative strength of one particular contribution term coupling the (axial) vectors to the (pseudo) scalars. {See Eq. (41) in [6].} In our setup there is a fixed link, Eq. (45), between the masses M_a and M_ρ and the pion decay constant f_π . This is the reason why here fixing f_π to its physical value constrains the axial vector mass from below. In Ref. [6] another term (with relative strength r_3) influences f_π and the direct impact of fixing f_π to its physical value on the axial mass is softened.

B. Beyond minimal walking technicolour

In Ref. [4] other models beyond minimal walking technicolour were listed systematically. These are viable candidates for dynamical electroweak symmetry breaking, as they may display a sufficiently large amount of walking and are not at odds with electroweak precision data. In view of the present computation they are characterised by the number of techniflavours N_f and the dimension d_R of the representation R of the gauge group under which the techniquarks transform. Conveniently, different values of these parameters lead only to rescalings of the axes of the plots in Fig. 1. Concretely, the masses are multiplied by $(3/d_R)^{1/2}$ and $(2/N_f)^{1/2}$. This scales the

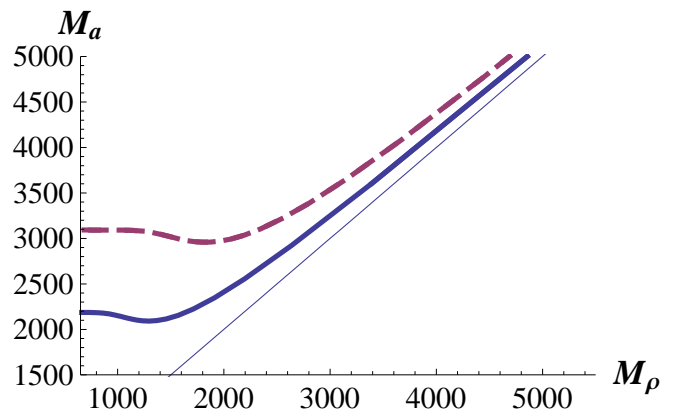


FIG. 3: M_a as function of M_ρ in the hard-wall model for minimal walking technicolour (dashed) and for the model with seven techniquarks (six of them gauged under the electroweak interactions) in the fundamental representation of $SU(2)$ (solid). The straight line indicates the value of M_ρ for comparison.

M_a graph downwards and the dip visible in the hard-wall model to the left when we increase d_R and/or N_f (see Fig. 3). In this context it is important to point out that N_f in this scaling is given by the number of techniflavours gauged under the electroweak group. First of all, this must be an even number to have complete doublets. Then it has proven to be advantageous to include more than two techniquarks to be close to conformality, while only gauging two under the electroweak gauge group to alleviate the bounds from electroweak precision data. For the *partially gauged* [3, 4] technicolour models, the number of gauged flavours is indicated in Tab. I in the column marked by N_f^g . As it turns out, of all models, the minimal mass for the axial vector meson in minimal walking technicolour is only surpassed in the partially gauged (two flavours gauged, seven overall) model with techniquarks in the fundamental representation of $SU(2)$. For all its sibling models the mass is reduced (see Tab. I).

The decay constants of the spin-one mesons scale differently, courtesy of the extra factor of g_5 in Eqs. (48) and (50). In both models and for vectors as well as axial vectors, the $F^{1/2}$ scale like $(3/d_R)^{1/4}$ and $(2/N_f)^{1/2}$. As measure for this scaling the rightmost column in Tab. I shows the square-root of the minimal value for the decay constant of the axial vector. It is achieved in the soft- as well as the hard-wall model when $M_\rho \rightarrow 0$.

Of all the models listed in Tab. I only those with techniquarks in the two-index symmetric representation of $SU(3)$ and $SU(4)$, respectively, feature the most basic flavour symmetry breaking pattern, that is $SU(2)_L \times SU(2)_R \rightarrow SU(2)_V$, which gives rise only to the (mesonic) fields contained in the action (1) and treated in detail in what followed.

All models with techniquarks in the adjoint representation possess two flavours irrespective of the number of colours. Thus, they are all covered exactly by the above

discussion up to the rescaling of the mass eigenvalues and decay constants treated in the present subsection.

The models with techniquarks in the fundamental representation of $SU(3)$ to $SU(6)$ and in the two-index symmetric representation of $SU(5)$ have an enlarged flavour symmetry due to their number of flavours N_f being larger than two, but not because of a (pseudo)real representation. Hence, we encounter $SU(N_f)_L \times SU(N_f)_R \rightarrow SU(N_f)_V$. The symmetry does not mix left and right fields. Consequently, we have only mesonic states among the (pseudo)scalars and (axial) vectors. The decomposition into vector and axial vector eigenstates is straightforward, $2V = A_L + A_R$ and $2A = A_L - A_R$.

The remaining model, seven flavours of the fundamental representation of $SU(2)$ as well as eight flavours of the two-index antisymmetric representation of $SU(4)$ feature enhanced symmetries due to the fact that they contain more than two flavours, but also because they feature pseudoreal and real representations, respectively. Hence, once more, part of the flavour symmetries involve mixing left and right handed fields and part of the extra spin-zero and spin-one states carry technibaryon number. Nevertheless, the spin-one particles are always either vector or axial vector eigenstates when described within the present framework. The exact decomposition involves handling $SU(14)$ or $SU(16)$ generators and is not performed here.

IV. SUMMARY

We have constrained the parameter space for the effective low-energy description for a set of walking technicolour models by imposing different variants of a holographic principle. In general, in such an effective action approach to strongly interacting theories, it is rather difficult to link the abundantly arising parameters to the less numerous parameters in the elementary theory. In the case of QCD, one can resort to experimental data. In beyond the standard model physics, this input is to date at best sparse. Here, one can fall back on a set of postulates which further constrain the model and can serve to enhance its predictive power. We chose two variants of a holographic principle. The holographic approaches have been adapted from Ref. [12] for the hard-wall model and Ref. [23] for the soft-wall model. The soft-wall model was introduced in order to model the equally spaced mass-squared eigenvalues known approximately from QCD (Regge trajectories) and expected in the presence of linear confinement. As it is not clear what to expect at the low-energy end for a quasi-conformal theory, especially for those with matter in the adjoint representation of the gauge group, we here simply compare the results from the hard- and the soft-wall scenario. There is accordance of these holographic descriptions with experimental values found for QCD, although QCD is a running theory and the holographic principle is based on a conjecture for a conformal theory. Clearly, there exists

no rigorous derivation for the here used low-energy description from the elementary theory. However, in view of the match achieved for QCD, a better accordance may be expected for the almost conformal technicolour theories we are concerned with. Seeing the potentially achievable predictive power, efforts towards the better understanding of the correspondence would appear to be a good investment.

The technicolour models were taken from the list of models which in Ref. [4] have been identified as viable candidates for breaking the electroweak symmetry dynamically, passing currently available electroweak precision tests. Among these is also the prime candidate, minimal walking technicolour, with two techniquarks transforming under the adjoint representation of $SU(2)$.

In the present approach the results obtained for mass eigenvalues and decay constants can be linked by scaling laws linking the results between different theories and we can concentrate on a single one in this synopsis. The masses scale like $d_R^{-1/2}$ with the representation of the technicolour group with respect to which the techniquarks transform and like $N_f^{-1/2}$ with the number of flavours. The square-roots of the decay constants, which in the conventions used here have the dimension of mass, scale like $d_R^{-1/4}$ and again like $N_f^{-1/2}$. For small vectorial masses the axial vector mass is bounded from below; in minimal walking technicolour at about 3 TeV and changed according to the scaling laws for the others (see Tab. I and Fig. 3). For large values of the vectorial mass also the mass of the lightest axial vector rises, becomes ever closer to the vector mass, but never falls below it (see Fig. 1). For a light first vector resonance also the second or even more vectors may be lighter than the first axial vector.

The predictions for the decay constants also differ somewhat between the two setups. In the soft-wall model the square-roots of the decay constants are linear functions of the corresponding mass with the same slope and zero intercept. In the hard-wall model for the vector, the relation is also linear with zero intercept, but larger slope. There, for the lowest possible values of the mass, the axial vector decay constant starts out with a value close to the soft-wall model and approaches the vector result in the hard-wall model from below for large values of the mass.

In other descriptions based on less and/or differently constrained effective low-energy actions these features can be different. For example for the setup in Refs. [6, 7] also inverted mass hierarchies can be found, with the first axial vector lighter than the first vector. In the range where the axial vector is as heavy as 3 TeV or heavier, the mass hierarchy is, however, predicted to be the normal one. In our approach fixing the pion decay constant to its physically required value automatically puts a lower bound on the axial vector mass. In the other approach, this is buffered by the larger number of parameters. As outlook, it would be interesting to investigate the role the corresponding terms play when combined with a holo-

graphic recipe. Further, the inclusion of non-zero quark masses may prove insightful.

Acknowledgments

The authors would like to thank Roshan Foadi, Mads T. Frandsen, Deog-Ki Hong, Matti Järvinen, and

Francesco Sannino for discussions. The work of DDD was supported by the Danish Natural Science Research Council. The work of CK was supported by the Marie Curie Fellowship under contract MEIF-CT-2006-039211.

-
- [1] S. Weinberg, *Phys. Rev. D* **19**, 1277 (1979);
L. Susskind, *Phys. Rev. D* **20**, 2619 (1979).
- [2] B. Holdom, *Phys. Rev. D* **24**, 1441 (1981);
K. Yamawaki, M. Bando and K. i. Matumoto, *Phys. Rev. Lett.* **56**, 1335 (1986);
T. W. Appelquist, D. Karabali and L. C. R. Wijewardhana, *Phys. Rev. Lett.* **57**, 957 (1986);
V. A. Miransky and K. Yamawaki, *Phys. Rev. D* **55**, 5051 (1997) [Erratum-ibid. *D* **56**, 3768 (1997)] [arXiv:hep-th/9611142];
V. A. Miransky, T. Nonoyama and K. Yamawaki, *Mod. Phys. Lett. A* **4**, 1409 (1989);
K. D. Lane and E. Eichten, *Phys. Lett. B* **222**, 274 (1989);
E. Eichten and K. D. Lane, *Phys. Lett. B* **90**, 125 (1980).
- [3] D. D. Dietrich, F. Sannino and K. Tuominen, *Phys. Rev. D* **73** (2006) 037701 [arXiv:hep-ph/0510217];
Phys. Rev. D **72** (2005) 055001 [arXiv:hep-ph/0505059];
F. Sannino and K. Tuominen, *Phys. Rev. D* **71** (2005) 051901 [arXiv:hep-ph/0405209].
- [4] D. D. Dietrich and F. Sannino, *Phys. Rev. D* **75** (2007) 085018 [arXiv:hep-ph/0611341].
- [5] S. B. Gudnason, C. Kouvaris and F. Sannino, *Phys. Rev. D* **73**, 115003 (2006) [arXiv:hep-ph/0603014].
- [6] R. Foadi, M. T. Frandsen, T. A. Rytto and F. Sannino, *Phys. Rev. D* **76** (2007) 055005 [arXiv:0706.1696 [hep-ph]].
- [7] R. Foadi, M. T. Frandsen and F. Sannino, arXiv:0712.1948 [hep-ph];
R. Foadi and F. Sannino, arXiv:0801.0663 [hep-ph].
- [8] S. Weinberg, *Phys. Rev. Lett.* **18** (1967) 507.
- [9] M. E. Peskin and T. Takeuchi, *Phys. Rev. D* **46** (1992) 381.
- [10] T. Appelquist and F. Sannino, *Phys. Rev. D* **59** (1999) 067702 [arXiv:hep-ph/9806409].
- [11] J. M. Maldacena, *Adv. Theor. Math. Phys.* **2** (1998) 231 [Int. J. Theor. Phys. **38** (1999) 1113] [arXiv:hep-th/9711200].
- [12] J. Erlich, E. Katz, D. T. Son and M. A. Stephanov, *Phys. Rev. Lett.* **95** (2005) 261602 [arXiv:hep-ph/0501128].
- [13] L. Da Rold and A. Pomarol, *Nucl. Phys. B* **721** (2005) 79 [arXiv:hep-ph/0501218];
JHEP **0601** (2006) 157 [arXiv:hep-ph/0510268];
J. Hirn, N. Rius and V. Sanz, *Phys. Rev. D* **73** (2006) 085005 [arXiv:hep-ph/0512240].
- [14] See for example
H. Liu, K. Rajagopal and Y. Shi, arXiv:0803.3214 [hep-ph] and references therein.
- [15] See for example
S. J. Brodsky and G. F. de Teramond, arXiv:0804.3562 [hep-ph];
arXiv:0804.0452 [hep-ph];
arXiv:0802.0514 [hep-ph];
Phys. Rev. D **77** (2008) 056007 [arXiv:0707.3859 [hep-ph]] and references therein.
- [16] S. Furui and H. Nakajima, *Phys. Rev. D* **76**, 054509 (2007) [arXiv:hep-lat/0612009].
- [17] T. Appelquist, G. T. Fleming and E. T. Neil, arXiv:0712.0609 [hep-ph].
- [18] D. K. Hong and H. U. Yee, *Phys. Rev. D* **74** (2006) 015011 [arXiv:hep-ph/0602177].
- [19] J. Hirn and V. Sanz, *Phys. Rev. Lett.* **97** (2006) 121803 [arXiv:hep-ph/0606086];
C. D. Carone, J. Erlich and J. A. Tan, *Phys. Rev. D* **75** (2007) 075005 [arXiv:hep-ph/0612242];
C. D. Carone, J. Erlich and M. Sher, *Phys. Rev. D* **76** (2007) 015015 [arXiv:0704.3084 [hep-th]].
- [20] S. Catterall and F. Sannino, *Phys. Rev. D* **76**, 034504 (2007) [arXiv:0705.1664 [hep-lat]].
- [21] L. Del Debbio, M. T. Frandsen, H. Panagopoulos and F. Sannino, arXiv:0802.0891 [hep-lat].
- [22] J. Polchinski and M. J. Strassler, arXiv:hep-th/0003136; *Phys. Rev. Lett.* **88** (2002) 031601 [arXiv:hep-th/0109174].
- [23] A. Karch, E. Katz, D. T. Son and M. A. Stephanov, *Phys. Rev. D* **74** (2006) 015005 [arXiv:hep-ph/0602229].
- [24] C. T. Hill and E. H. Simmons, *Phys. Rept.* **381**, 235 (2003) [Erratum-ibid. **390**, 553 (2004)] [arXiv:hep-ph/0203079].
- [25] M. A. Stephanov, *Phys. Rev. D* **76** (2007) 035008 [arXiv:0705.3049 [hep-ph]].
- [26] M. Abramovitz and I. A. Stegun, “Handbook of Mathematical Functions.”
- [27] See for example footnote #18 on p.86 in F. Sannino, arXiv:0804.0182v1 [hep-ph].
- [28] S. B. Gudnason, C. Kouvaris and F. Sannino, *Phys. Rev. D* **74**, 095008 (2006) [arXiv:hep-ph/0608055].